Electronic Supplementary Information

Improving the Performance for Direct Electrolysis of CO_2 in Solid Oxide Electrolysis Cell with $Sr_{1.9}Fe_{1.5}Mo_{0.5}O_{6-\delta}$ Electrode via Infiltration of Pr_6O_{11} Nanoparticles

Wanhua Wang[a], Haixia Li[a], Clarita Y. Regalado Vera[b,c], Jie Lin[a], Ka-Young Park[a], Taehee Lee[a], Dong Ding[*b] and Fanglin Chen[*a]

[a]Department of Mechanical Engineering, University of South Carolina, Columbia, SC, 29208, USA.
[b]Energy & Environmental Science and Technology, Idaho National Laboratory, Idaho Falls, ID, 83415, USA.
[c]Department of Chemical & Materials Engineering, New Mexico state University, Las Cruses, NM, 88003, USA.

[*]Corresponding author: Email: dong.ding@inl.gov (D. D.); chenfa@cec.sc.edu (F. C.)

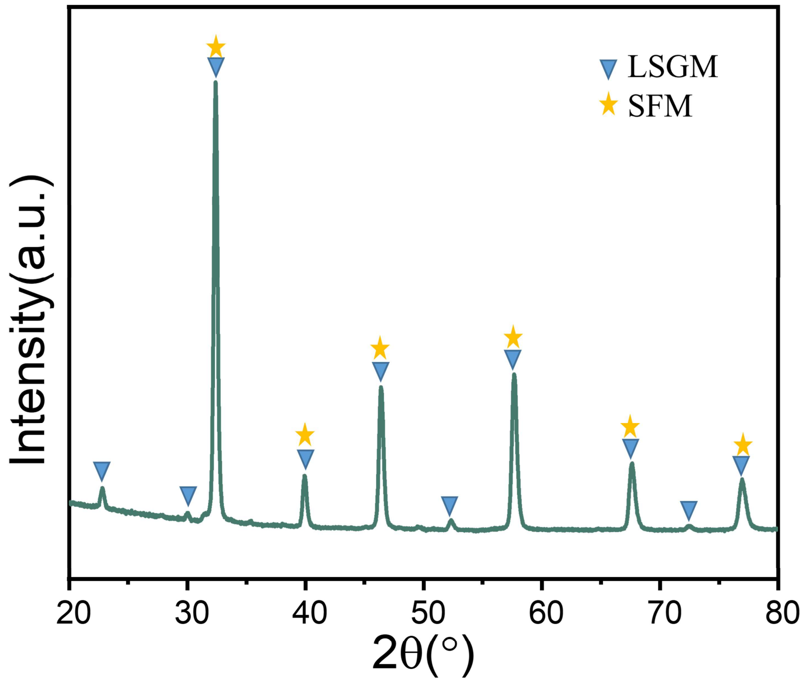

Figure S1. XRD profiles of the mixture powder of 50wt.%SFM with 50wt.%LSGM treated in air at 1000°C for 2h.

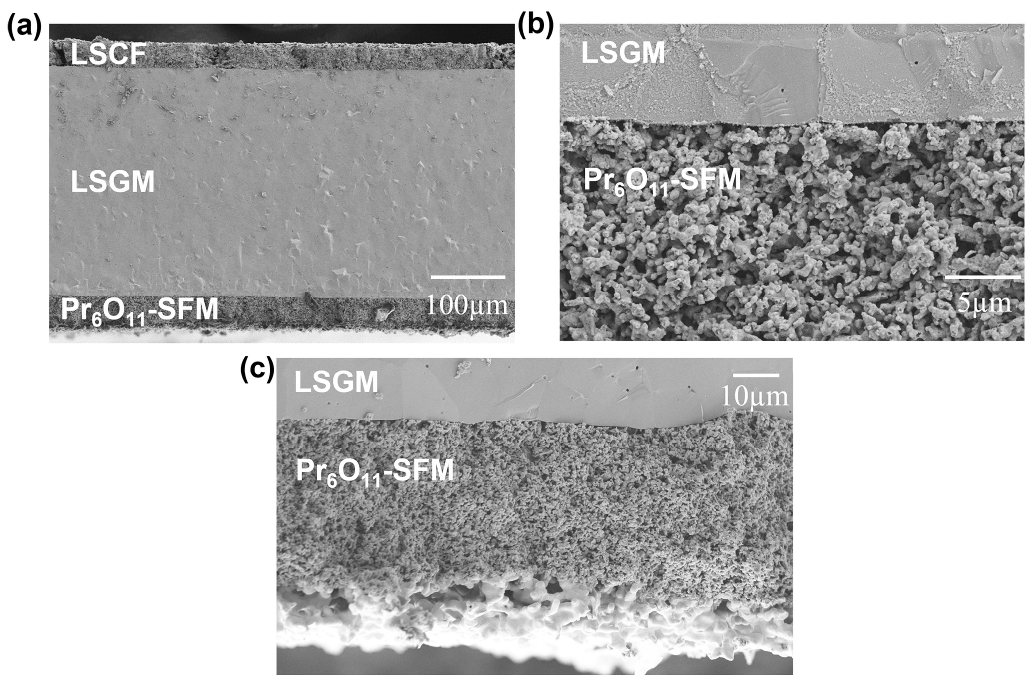

Figure S2. Cross-sectional microstructure of 14.8wt.%Pr_6O_{11}-SFM single cell. (a) The cross-section view of the entire cell, (b) the magnified cathode/electrolyte view before testing, (c) the cathode/electrolyte interface after long-term stability testing.

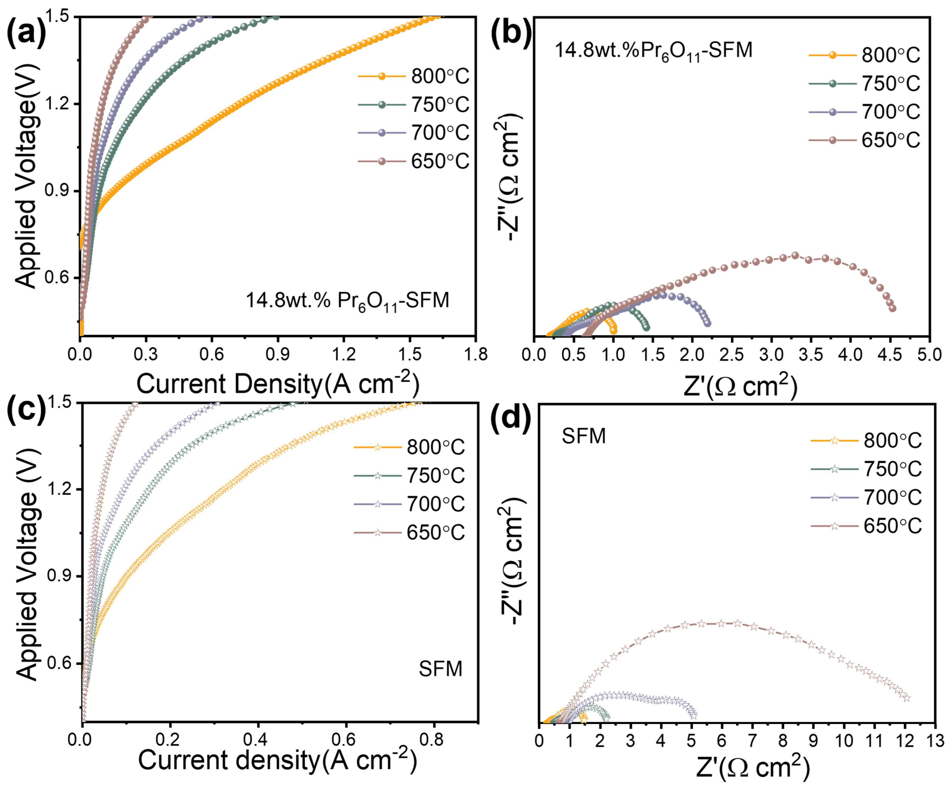

Figure S3. CO_2 electrolysis performance comparison of single cells with SFM and 14.8wt.%Pr_6O_{11}-SFM cathode, respectively. I-V curves (a) and EIS results (b) of 14.8wt.%Pr_6O_{11}-SFM single cells at different temperature. I-V curves (c) and EIS results (d) of SFM single cells at different temperature.

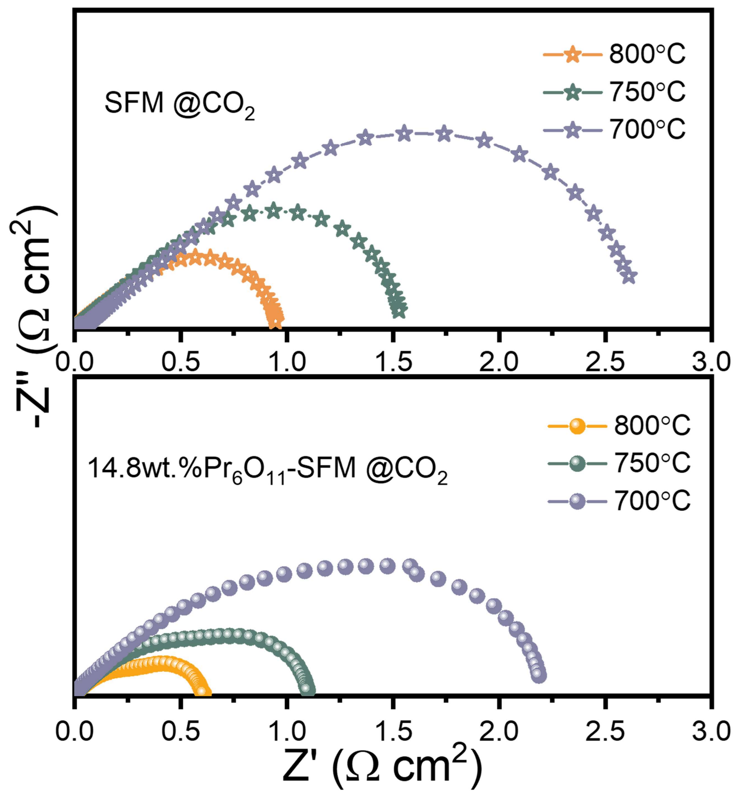

Figure S4. CO_2 electrolysis performance comparison of symmetrical cells with SFM and 14.8wt.%Pr_6O_{11}-SFM electrode at different temperature.

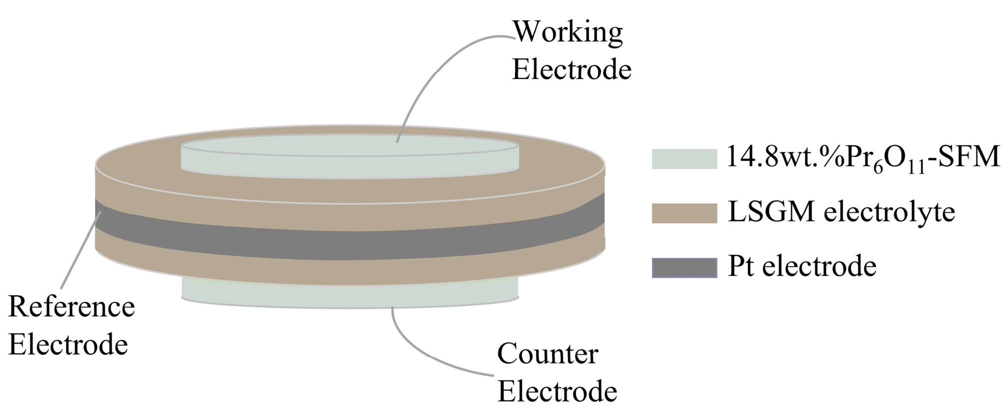

Figure S5. Schematic diagram of three-electrode cell.

Table S1. Performance comparison at 800°C for pure CO_2 electrolysis at 1.5V

Cell configuration Cathode/Electrolyte/Anode	**Electrolyte thickness (μm)**	**Current density (A/cm^2) at 1.5V**	**Polarization resistance (Ω cm^2) at OCV**	**Ref.**
LSCrM-SDC/YSZ/LSCrM-SDC	2000	0.10	3.1	S1
LSFT/YSZ/LSFT	700	0.28	--	S2
Ni@LSTM/YSZ/LSM^1-SDC	500	0.43	--	S3
LSFM-GDC/YSZ/LSFM-DC	200	0.51	0.85	S4
LSCFN-GDC/YSZ/LSCFN-GDC	200	0.442	0.683	S5
LSFN-GDC/YSZ/LSFN-GDC	400	0.55	0.12	S6
LSTMC/LSGM/LSM^2	350	1.24	0.311	S7
LSF/LSGM/LSCF-SDC	240	0.76	1.31	S8
12.8wt.%GDC-SFM/YSZ/LSM^3-YSZ	500	0.45	--	S9
SFM-YSZ/YSZ/LSM-YSZ	10	1.10	0.41	S10
SFM-SDC/LSGM/LSCF-SDC	230	1.09	0.512	S11
F-SFM/LSGM/LSCF-SDC	250	1.36	0.656	S12
SFMM-SDC/LSGM/LSCF-SDC	400	1.35	0.58	S13
SFM/LSGM/LSCF	310	0.76	1.38	This work
14.8wt.%Pr_6O_{11}-SFM/LSGM/LSCF	310	1.61	0.81	This work

LSCrM=$La_{0.75}Sr_{0.25}Cr_{0.5}Mn_{0.5}O_{3-\delta}$; SDC=$Ce_{0.8}Sm_{0.2}O_{2-\delta}$; GDC=$Ce_{0.8}Sm_{0.2}O_{2-\delta}$; LSFT= $La_{0.3}Sr_{0.7}Fe_{0.7}TiO_{3-\delta}$; LSTM= $La_{0.2}Sr_{0.8}Ti_{0.9}Mn_{0.1}O_{3+\delta}$; LSM^1= $(La_{0.8}Sr_{0.2})_{0.95}MnO_{3-\delta}$; LSFM= $La_{0.6}Sr_{0.4}Fe_{0.9}Mn_{0.1}O_{3-\delta}$; LSCF=$La_{0.6}Sr_{0.4}Co_{0.2}Fe_{0.8}O_{3-\delta}$; LSCFN=$La_{0.4}Sr_{0.6}Co_{0.2}Fe_{0.7}Nb_{0.1}O_{3-\delta}$; LSTMC=$(La_{0.2}Sr_{0.8})_{0.95}Ti_{0.55}Mn_{0.35}Cu_{0.1}O_{3-\delta}$; LSM^2=$La_{0.8}Sr_{0.2}MnO_{3-\delta}$; LSF=$La_{0.8}Sr_{0.2}FeO_{3-\delta}$; SFM= $Sr_2Fe_{1.5}Mo_{0.5}O_{6-\delta}$; LSM^3= $(La_{0.85}Sr_{0.15})_{0.9}Mn_{3-\delta}$; F-SFM=F-$Sr_2Fe_{1.5}Mo_{0.5}O_{6-\delta}$; SFMM=$Sr_2Fe_{1.4}Mn_{0.1}Mo_{0.5}O_{6-\delta}$;

Table S2: Polarization resistance values of 14.8wt.%Pr_6O_{11}-SFM and SFM electrodes under open circuit conditions in pure CO_2 atmosphere at different temperatures

Electrode	**R_p (Ω cm^2) at 800°C**	**R_p (Ω cm^2) at 750°C**	**R_p (Ω cm^2) at 700°C**
14.8wt.%Pr_6O_{11}-SFM	0.61	1.09	2.18
SFM	0.95	1.53	2.62

Notes and references

S1. S. Xu, S. Li, W. Yao, D. Dong and K. Xie, *J. Power Sources*, 2013, **230**, 115–121.

S2. Z. Cao, B. Wei, J. Miao, Z. Wang, Z. Lü, W. Li, Y. Zhang, X. Huang, X. Zhu, Q. Feng and Y. Sui, *Electrochem. commun.*, 2016, **69**, 80–83.

S3. L. Ye, M. Zhang, P. Huang, G. Guo, M. Hong, C. Li, J. T. S. Irvine and K. Xie, *Nat. Commun.*, 2017, **8**, 1–10.

S4. X. Peng, Y. Tian, Y. Liu, W. Wang, L. Jia, J. Pu, B. Chi and J. Li, *J. CO2 Util.*, 2020, **36**, 18–24.

S5. Z. Yang, C. Ma, N. Wang, X. Jin, C. Jin and S. Peng, *J. CO2 Util.*, 2019, **33**, 445–451.

S6. Y. Tian, H. Zheng, L. Zhang, B. Chi, J. Pu and J. Li, *J. Electrochem. Soc.*, 2018, **165**, F17.

S7. X. Yang, K. Sun, M. Ma, C. Xu, R. Ren, J. Qiao, Z. Wang, S. Zhen, R. Hou and W. Sun, *Appl. Catal. B Environ.*,2020, **272**, 118968.

S8. Y. Yang, Y. Li, Y. Jiang, M. Zheng, T. Hong, X. Wu and C. Xia, *Electrochim. Acta*, 2018, **284**, 159–167.

S9. H. Lv, Y. Zhou, X. Zhang, Y. Song, Q. Liu, G. Wang and X. Bao, *J. Energy Chem.*, 2019, **35**, 71–78.

S10. Y. Li, P. Li, B. Hu and C. Xia, *J. Mater. Chem. A*, 2016, **4**, 9236–9243.

S11. Y. Li, X. Chen, Y. Yang, Y. Jiang and C. Xia, *ACS Sustain. Chem. Eng.*, 2017, **5**, 11403–11412.

S12. Y. Li, Y. Li, Y. Wan, Y. Xie, J. Zhu, H. Pan, X. Zheng and C. Xia, *Adv. Energy Mater.*, 2019, **9**, 1803156.

S13. Y. Jiang, Y. Yang, C. Xia and H. J. M. Bouwmeester, *J. Mater. Chem. A*, 2019, **7**, 22939–22949.